Smart Structures and Systems, *Vol. 14, No. 4 (2014) 699-718*
DOI: http://dx.doi.org/10.12989/sss.2014.14.4.699

Extension of indirect displacement estimation method using acceleration and strain to various types of beam structures

Soojin Cho[1], Sung-Han Sim[*1], Jong-Woong Park[2] and Junhwa Lee[1]

[1]*School of Urban and Environmental Engineering, Ulsan National Institute of Science and Technology, Ulsan 689-798, South Korea*
[2]*Department of Civil and Environmental Engineering, University of Illinois at Urbana-Champaign, Urbana 61801, IL, USA*

(Received May 30, 2014, Revised August 20, 2014, Accepted August 30, 2014)

Abstract. The indirect displacement estimation using acceleration and strain (IDEAS) method is extended to various types of beam structures beyond the previous validation on the prismatic or near-prismatic beams. By fusing different types of responses, the IDEAS method is able to estimate displacements containing pseudo-static components with high frequency noise to be significantly reduced. However, the concerns to the IDEAS method come from possible disagreement of the assumed sinusoidal mode shapes to the actual mode shapes, which allows the IDEAS method to be valid only for simply-supported prismatic beams and limits its applicability to real world problems. In this paper, the extension of the IDEAS method to the general types of beams is investigated by the mathematical formulation of the modal mapping matrix only for the monitored substructure, so-called *monitoring span*. The formulation particularly considers continuous and wide beams to extend the IDEAS method to general beam structures that reflect many real bridges. Numerical simulations using four types of beams with various irregularities are presented to show the effectiveness and accuracy of the IDEAS method in estimating displacements.

Keywords: displacement; acceleration; strain; data fusion; beam structure

1. Introduction

Civil infrastructure is the national asset that supports diverse activities of the public. Since their obsolete function brings considerable economic loss in the society, structural health of the infrastructure needs to be continuously monitored. Various efforts have been placed to monitor the structural health in efficient and inexpensive way: majority of them used acceleration as the measurement, since acceleration can be processed to the modal information (e.g., natural frequencies, modal damping ratios, and mode shapes) that helps to assess the health comprehensively (Doebling *et al*. 1998, Yi *et al*. 2007, Bani-Hani *et al*. 2008, Altunisik *et al*. 2012, Kim *et al*. 2013).

Displacement is an intuitive response that results from the forces applied to a structural system. For a linear structure, its displacement satisfies Hooke's law and can reveal the stiffness of the structure with the given force. Even in the case of a nonlinear structure, the displacement can be

∗Corresponding author, Assistant Professor, E-mail: ssim@unist.ac.kr

http://www.techno-press.org/?journal=sss&subpage=8 ISSN: 1738-1584 (Print), 1738-1991 (Online)

represented by nonlinear relationship between the applied force and the structure. Thus, based on the relationship, a displacement is regarded as a useful indicator for not only the integrity but also the serviceability of a structure (Zhou *et al*. 2013).

Many devices have been developed to measure the displacement in the direct manner, and the most famous one would be the linear variable differential transformers (LVDT). The big challenge of direct displacement measurement is a fixed reference point where the devices should stand still regardless of the deformation of the host structure. The need of the reference point critically limits the usage of the direct measurement devices at civil structures, such as bridges, skyscrapers, and dams, which are very hard to find the reference points around them. Recently, non-contact type devices, such as global positioning systems (GPS), laser Doppler vibrometers (Nassif *et al*. 2005), and vision-based systems (Lee and Shinozuka 2006, Ye *et al*. 2013) have emerged to clear the hurdle at the civil structures. Though the non-contact property helps to dodge the difficulty in finding good reference point, the high equipment cost significantly limits the number of measurement points, preventing their wider adoption in practice.

Beyond the use of the non-contact type devices, there have been many efforts to indirectly estimate the displacement from the other responses that can be easily captured: such as acceleration and strain. The acceleration is an absolute measure and which does not require the reference point, and its double integration is considered to be the displacement. Though the literatures (Ribeiro *et al*. 1997, Park *et al*. 2005, Jung *et al*. 2006, Gindy *et al*. 2008, Lee *et al*. 2010, Kandula *et al*. 2012, Ma *et al*. 2014) show successful results, the acceleration-based approaches have the inherent limitation; they cannot estimate pseudo-static components of the dynamic displacement that accelerometers cannot capture. The strain is another effective response that can be converted into the dynamic displacement including the pseudo-static component. Foss and Hauge (1995) proposed a strain-displacement modal mapping method to transform a number of discrete strain measurements into dynamic displacement using modal properties of a structure, and the modal mapping method is used widely to convert the strain to displacement (Kang *et al*. 2007, Shin *et al*. 2012). The strain does not cause the drift; however, the estimated displacement is vulnerable to measurement noise especially in the high frequency range, and it requires preliminary tests for calibration of neutral axis of the beam structure (Shin *et al*. 2012).

The respective weaknesses of the indirect estimation methods using either acceleration or strain can be strengthened by the fused use of them. Park *et al*. (2013) proposed an indirect displacement estimation using acceleration and strain (IDEAS) method by combining an acceleration-based method (Lee *et al*. 2010) with strain-based modal mapping method using assumed mode shapes (Shin *et al*. 2012). The IDEAS method was shown to successfully estimate displacement responses of single-span simply-supported structures that contain both dynamic and pseudo-static components. Though a three-span suspension bridge is used in the experimental test, the mode shapes of the bridge are assumed to be similar to the sinusoidal mode shapes as in a single-span simply-supported beam.

This paper aims to investigate the extendibility of the IDEAS method to various types of beam structures which are expected to have non-sinusoidal mode shapes. In practice, the bridge, which is the representative beam-type civil structure, does not have a prismatic section and/or a single span, and it does not have the mode shapes that are exactly sinusoidal. The IDEAS method constructs the modal mapping matrix using the assumed sinusoidal mode shapes, and thus, the disagreement between the assumed and real mode shapes can be a significant error-causing factor in the estimation of the displacement. In this paper, the IDEAS method is extended to the general types of beams based on the mathematical formulation of modal mapping matrix using the sinusoidal mode shapes. The extendibility of the IDEAS method is accomplished by constructing the modal mapping matrix only for the monitored substructure, so-called *monitoring span* in this paper. To validate the extension, the IDEAS method is implemented to four numerical beam models: (1) a single-span beam with non-prismatic section, (2) a single-span beam with asymmetric section, (3) a two-span beam with prismatic section, and (4) a two-span beam with asymmetric sections. The displacement estimated by the IDEAS method is compared with the exact displacement as well as the estimated displacements by the acceleration-based and strain-based methods (Lee *et al*. 2010, Shin *et al*. 2012), and the robustness of the IDEAS method to the general types of beams is investigated.

2. Indirect displacement estimation using acceleration and strain (IDEAS)

This section describes the principles of the acceleration-based displacement estimation method (Lee *et al*. 2010), strain-based displacement estimation method (Shin *et al*. 2012), and the IDEAS method. Then the motivation of the study arisen from the principles will be stated.

2.1 Acceleration-based displacement estimation method

The displacement estimation method using the acceleration proposed by Lee *et al*. (2010) is the starting point of the IDEAS method. This method estimates the displacement by solving the optimization problem as

$$\underset{u}{\mathrm{Min}}\,\Pi = \frac{1}{2}\left\| L_a (L_c u - (\Delta t)^2 \overline{a}) \right\|_2^2 + \frac{\lambda^2}{2}\left\| u \right\|_2^2 \tag{1}$$

where u and $\overline{a}$ are the estimated displacement and the measured acceleration vectors in discrete time domain, respectively; L_a is a diagonal weighting matrix having the first and last entries as $1/\sqrt{2}$ and the other entries as 1; L_c is the second-order differential operator matrix of the discretized trapezoidal rule (Atkinson 2008); $\|\cdot\|_2$ is 2-norm of a vector; Δt is the time step; λ is a regularization factor. The first term in the right-hand-side of Eq. (1) represents the error between the measured acceleration and the second-order derivative of the estimated displacement. The second term (i.e., regularization term) is introduced to remove out the possible signal drift. The solution of Eq. (1) is

$$u = (L^T L + \lambda^2 I)^{-1} L^T L_a \overline{a} (\Delta t)^2 = C_a \overline{a} (\Delta t)^2 \tag{2}$$

where $L = L_a L_c$ and $C_a = (L^T L + \lambda^2 I)^{-1} L^T L_a$.

The above minimization problem in Eq. (1) is Tikhonov regularization scheme and the λ in Eq. (2) is the regularization factor that adjusts the degree of the regularization in the minimization problem. As the regularization factor becomes larger, the solution bound approaches zero, and zero displacements are reconstructed. λ is optimally defined by Lee *et al*. (2010) as

$$\lambda = 46.81 N_d^{-1.95} \tag{3}$$

where N_d is the size of the time-window, in which the acceleration data to be processed into displacement at a time. Short time-window can reduce computational effort for data processing while sacrificing the accuracy. The optimal size of the time-window can be determined based on the natural frequencies of a structure; more practical way in the rule of thumb is to use three times of the number of data points in the first natural period for a time-window, which exhibits reasonable accuracy in the estimation. More details can be found in Lee *et al*. (2010).

The estimated displacement causes significant error near both ends of the finite data, since the axiom that acceleration equals to the second-order derivative of displacement is valid only when the boundary conditions on velocity and displacement are provided. To resolve this issue, an overlapping moving window strategy is taken as shown in Fig. 1. For a given finite acceleration data, only the data with a moving time-window by Δt is processed by Eq. (2) sequentially, and the estimated displacements at the center of the moving time-windows are connected in series to construct the whole estimated displacement.

2.2 Strain-based displacement estimation method

The dynamic displacement can also be estimated from the measured dynamic strain using the strain-displacement modal mapping method (Foss and Hauge 1995). The displacement and strain measurements can be expressed using the modal superposition as

$$u_{m\times 1} = \Phi_{m\times r} q_{r\times 1} \tag{4}$$

$$\varepsilon_{n\times 1} = \Psi_{n\times r} q_{r\times 1} \tag{5}$$

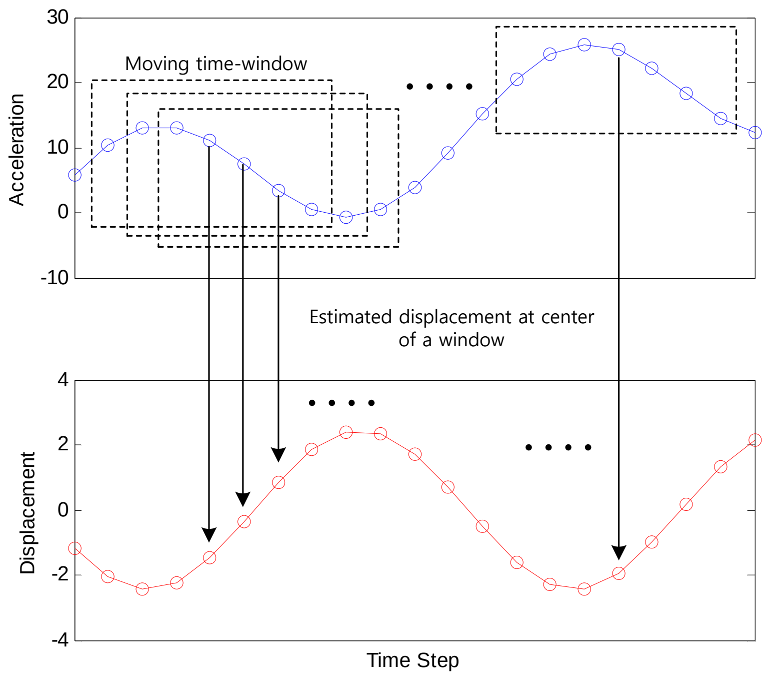

Fig. 1 Displacement estimation using moving time-window (modified from Lee *et al*. (2010))

where ε is the measured strain vector; Φ and Ψ are the displacement and strain mode shape matrices, respectively; q is the modal coordinate vector; m and n is the number of measurements for the displacement and the strain, respectively; and r is the number of used modes. When $n \geq r$, the displacement can be expressed using the strain as

$$u = D_{m\times n}\varepsilon \tag{6}$$

$$D_{m\times n} = \Phi\Psi^{\dagger} \tag{7}$$

where the superscript † denotes the Moore-Penrose pseudo inverse; and D is the mapping matrix from strain to displacement obtained as a least-squared solution.

Shin *et al*. (2012) have used the assumed mode shapes, appeared as sinusoidal form, for single-span simply-supported beam structures as

$$\Phi = \begin{bmatrix} \sin\frac{\pi x_1}{L} & \cdots & \sin\frac{r\pi x_1}{L} \\ \vdots & \ddots & \vdots \\ \sin\frac{\pi x_n}{L} & \cdots & \sin\frac{r\pi x_n}{L} \end{bmatrix} \tag{8}$$

$$\Psi = \frac{y\pi^2}{L^2}\begin{bmatrix} \sin\frac{\pi x_1}{L} & \cdots & r^2\sin\frac{r\pi x_1}{L} \\ \vdots & \ddots & \vdots \\ \sin\frac{\pi x_n}{L} & \cdots & r^2\sin\frac{r\pi x_n}{L} \end{bmatrix} \tag{9}$$

By combining Eqs. (8) and (9), the mapping matrix can be constructed as

$$D = \frac{L^2}{y\pi^2}\begin{bmatrix} \sin\frac{\pi x_1}{L} & \cdots & \sin\frac{r\pi x_1}{L} \\ \vdots & \ddots & \vdots \\ \sin\frac{\pi x_n}{L} & \cdots & \sin\frac{r\pi x_n}{L} \end{bmatrix}\begin{bmatrix} \sin\frac{\pi x_1}{L} & \cdots & r^2\sin\frac{r\pi x_1}{L} \\ \vdots & \ddots & \vdots \\ \sin\frac{\pi x_n}{L} & \cdots & r^2\sin\frac{r\pi x_n}{L} \end{bmatrix}^{\dagger} \tag{10}$$

where L is length of the beam structure; $x_i (i = 1, \cdots, n)$ is the measurement location of strain; y is neutral axis of the beam; and r is the number of used modes.

2.3 Indirect Displacement Estimation Using Acceleration and Strain (IDEAS)

Park *et al*. (2013) have proposed the IDEAS method by fusing the aforementioned two methods. Using the modal mapping matrix in Eq. (10), the optimization problem in Eq. (1) is modified for displacement u_i at the location of x_i as

$$\underset{u_i}{\text{Min}}\,\Pi = \frac{1}{2}\left\| L_a (L_c u_i - (\Delta t)^2 \overline{a}_i) \right\|_2^2 + \frac{\lambda^2}{2}\left\| u_i - D_i \overline{\varepsilon} \right\|_2^2 \tag{11}$$

where D_i is the i th row of D in Eq. (10); $\overline{\varepsilon}$ is the measured strain; u_i and $\overline{a}_i$ are the estimated displacement and measured acceleration at the location x_i. Eq. (11) uses the measured strain to remove out the drift instead of using regularization term of Eq. (1).

The solution of Eq. (11) can be expressed as

$$\begin{aligned} u_i &= (L^T L + \lambda^2 I)^{-1}(L^T L_a \overline{a}_i \Delta t^2 + \lambda^2 D_i \overline{\varepsilon}) \\ &= \begin{pmatrix} C_a \Delta t^2 & C_\varepsilon \end{pmatrix} \begin{pmatrix} \overline{a}_i \\ \overline{\varepsilon} \end{pmatrix} \end{aligned} \tag{12}$$

where $C_\varepsilon = (L^T L + \lambda^2 I)^{-1} \lambda^2 D_i$.

In Eq. (7), r should be smaller than n to avoid under-determined modal mapping matrix, while taking smaller n (i.e., using small number of strain gauges) is preferable. In the rule of thumb, the first three modes are utilized to estimate the displacement with reasonable accuracy considering the facilitation of obtaining the lower modes in the field (Koo *et al*. 2010, Park *et al*. 2013), which specifies the minimum number of strain measurements as three.

The strain measurement involves an inherent problem, which is the determination of neutral axis. Generally, the neutral axis is calculated from the drawing or the finite element model. However, complexity of a structure due to composite materials (e.g., reinforced concrete) or irregular cross section makes the calculation difficult. A simple calibration procedure using acceleration and strain signals is proposed by Park *et al*. (2013) as

$$\alpha = \sqrt{\frac{S_{d,acc}(f_c)}{S_{d,str}(f_c)}} \tag{13}$$

where α is the scaling factor which converts the measured strain into the strain measured at the neutral axis, $S_{d,acc}$ and $S_{d,str}$ are the power spectral densities (PSD) of the displacements estimated from acceleration and strain using Eqs. (1) and (6), and f_c is a selected natural frequency that is clearly apparent from the both displacements estimated from acceleration and strain. Since both acceleration and strain can capture the first mode with high accuracy, the first mode is a good candidate for f_c. If the other mode, such as the second or third mode, has high amplitude in the frequency domain, it also can be used as f_c.

3. Extension of IDEAS method

Rooted in the strain-based approach described previously, the current IDEAS method is seemingly limited to simply-supported beam structures that have the sinusoidal mode shapes. The IDEAS method constructs the modal mapping matrix using the assumed sinusoidal mode shapes, and thus possible disagreement of the assumed sinusoidal mode shapes, used in Eqs. (8) and (9), to the real mode shapes of the structure can cause a significant error in the estimation of displacement. In the paper by Park *et al*. (2013), the validation was carried out on a simply-supported beam in the numerical simulation and a suspension bridge in the experiment. Both structures have prismatic or nearly-prismatic sections and large span-to-depth ratios, and thus have the mode shapes quite close to the assumed mode shapes. However, in practice, such assumed mode shapes are suspected to be invalid particularly for non-prismatic beams, wide beams, and continuous beams. In such cases, the sinusoidal mode shapes can be a primary source of errors in the displacement estimation. The errors can be removed out by performing the modal testing using a dense array of accelerometers and strain gauges, but it is too costly and time-consuming. Therefore, if the error caused from the assumption of sinusoidal functions is reasonably acceptable even for the general beams, the replacement of expensive modal testing would still be very attractive.

This section describes the extension of the IDEAS method to the general beams based on the mathematical formulation of modal mapping matrix using the sinusoidal mode shapes. The extension is based on the fact that the modal mapping matrix can be composed using both deflection and strain mode shapes of a substructure at which displacement is estimated. In this paper, a single span between two supports is considered as the substructure, which will be called as a *monitoring span* throughout this paper.

Consider the case of estimating displacement from a general beam structure with varying sections, overhanging members, and/or multiple spans. The actual mode shapes of a *monitoring span* would be discrepant from the sinusoidal functions, unlikely to the prismatic simply-supported beams. The actual mode shapes can be obtained from the modal testing using a dense array of sensors. However, the sinusoidal functions of a few largest wave lengths still constitute an acceptable modal mapping matrix for the *monitoring span* without costly modal testing. Though the sinusoidal functions bring the error in converting strain to displacement, the use of acceleration in the IDEAS method, shown in Eq. (12), counterbalances the total error in the estimated displacement, which will be demonstrated in the numerical simulations.

The IDEAS method using a few sinusoidal functions is still valid for the beams whose mode shapes are appeared to be similarly repeated at the *monitoring span*, such as continuous beams with multiple spans and wide beams. To visually show the idea, the first two mode shapes of a 2-span continuous beam are depicted in Fig. 2. For the whole length of $2l$, these two mode shapes are orthogonal to each other. Limited to a *monitoring span* with the length of l, however, the mode shapes are similar to each other as well as to the sinusoidal function of the largest wave length (i.e., $\sin(\pi x/l)$ $(0 \le x \le l)$). If the number of span is increasing, the similar mode shapes at a *monitoring span* will increasingly appear. Therefore, a set of repeated sinusoidal functions of a few largest wave lengths can constitute an acceptable modal mapping matrix of the *monitoring span*.

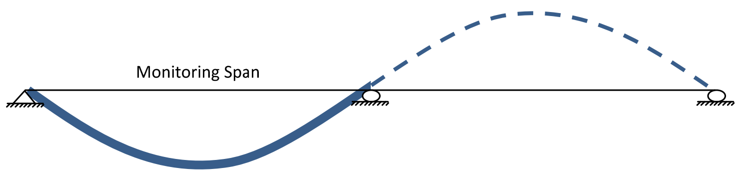

(a) First mode shape

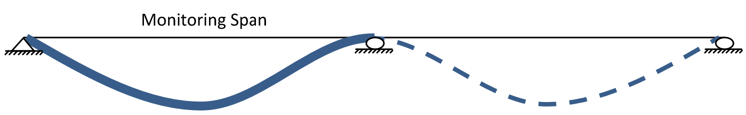

(b) Second mode shape

Fig. 2 First two mode shapes of a two-span continuous beam

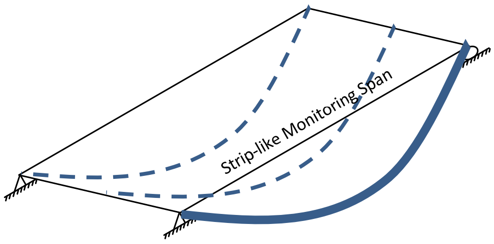

(a) First bending mode shape

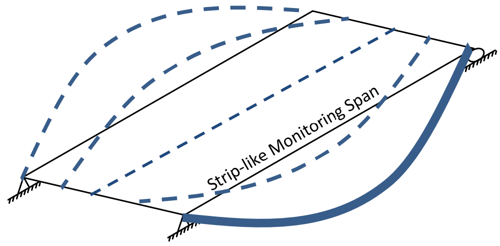

(b) First torsional mode shape

Fig. 3 First bending and torsional mode shapes of a wide beam

The modal mapping matrix using a set of repeated sinusoidal functions can be simplified to the modal mapping using the sinusoidal functions without repetition. This simplification provides mathematical background in applying the IDEA method to various types of beam structures whose mode shapes in a monitored span are similarly repeated. If a set of r sinusoidal functions $\{\phi_1,\cdots,\phi_k,\cdots,\phi_r\}$ are assumed for the mode shapes, the modal mapping matrix D can be defined as the Eq. (10). Assume that a repeated sinusoidal function ϕ_k is included in the set, making the set of assumed mode shapes as $\{\phi_1,\cdots,\phi_k,\phi_k,\cdots,\phi_r\}$ and the set of assumed strain mode shapes as $\{\psi_1,\cdots,\psi_k,\psi_k,\cdots,\psi_r\}$.Since ϕ_k can be substituted to $D\psi_k$ only when $k=1,...,r$, the new modal mapping matrix $\bar{D}$ can be simplified to the original modal mapping matrix D as

$$\begin{aligned}\bar{D} &= [\phi_1 \ \cdots \ \phi_k \ \phi_k \ \cdots \ \phi_r][\psi_1 \ \cdots \ \psi_k \ \psi_k \ \cdots \ \psi_r]^{\dagger} \\ &= [D\psi_1 \ \cdots \ D\psi_k \ D\psi_k \ \cdots \ D\psi_r][\psi_1 \ \cdots \ \psi_k \ \psi_k \ \cdots \ \psi_r]^{\dagger} \\ &= D[\psi_1 \ \cdots \ \psi_k \ \psi_k \ \cdots \ \psi_r][\psi_1 \ \cdots \ \psi_k \ \psi_k \ \cdots \ \psi_r]^{\dagger} \\ &= D\end{aligned} \tag{14}$$

Therefore, by using a sufficient number of assumed modes, the modal mapping matrix of a beam with repeated mode shapes at a *monitoring span* can be easily constructed.

This proposition can be applied to wide beams that have torsional mode shapes, which can be approximated as sinusoidal mode shapes at a *strip-like monitoring span* as shown in Fig. 3. More detailed strategy for the extension of IDEAS method using sinusoidal functions will be discussed in the following section with numerical examples.

4. Numerical validation

The numerical validation of the extension of the IDEAS method will be carried out on four examples that have varying sections and/or multiple spans. Two examples – non-prismatic and asymmetric single-span beams – are developed with expectation of non-sinusoidal mode shapes. Another example is a two-span prismatic beam that will have repeated mode shapes when only a single span is measured. The last example is a two-span beam with asymmetric sections which is expected to have the non-sinusoidal and the repeated mode shapes at an observed single span.

4.1 Common simulation setup

All models used in this study are the variations of the single-span prismatic beam model shown in Fig. 4. The beam model is composed of Euler-Bernoulli beam elements with rectangular sections. N# and A# in Fig. 4 denote nodes and supports, respectively. The variations are made on the depth of the rectangular section and the number of spans. The length, width, Young's modulus, and mass density of the beam elements are kept same as the Park *et al*. (2013). Table 1 tabulates the details of the beam model.

The responses – displacement, acceleration, and strain – of the model are simulated using MATLAB Simulink. A vertical moving load used in the Park *et al*. (2013) is again employed to excite the beam model for this study: it moves from the left to the right with a constant velocity (v =0.1 m/s) to generate non-zero mean displacements as shown in Fig. 5. The moving load is the combination of static load of 10N and zero-mean Gaussian random load with the standard deviation of 3N. Given N5 of Fig. 4 as the test point, the acceleration is measured at the node N5, while the strains are obtained at three nodes of N4, N8, and N12. The exact displacement of N5 is also obtained to be used as reference data. The acceleration and strain are contaminated by adding 5% and 10% noise in RMS (root mean square), respectively, to simulate the practical measurement.

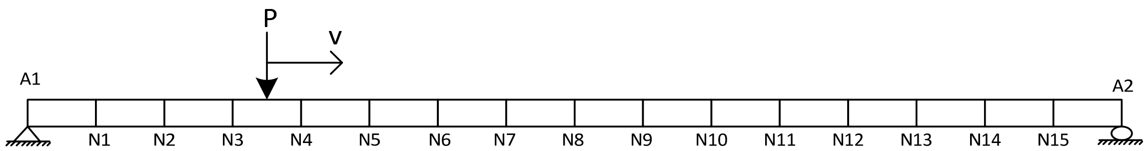

Fig. 4 Single-span prismatic beam model

Table 1 Details of the prismatic beam model (Park *et al*. 2013)

Element length	0.1 m
Element width	0.015 m
Young's modulus	206 GPa
Mass density	7850 kg/m^3
Element depth	0.004 m for the prismatic beam (variations made in this study)

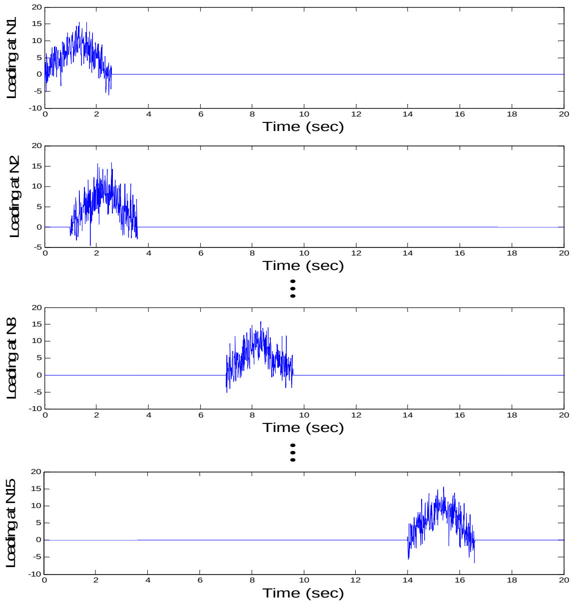

Fig. 5 Simulated vertical moving load (Park *et al*. 2013)

4.2 Single-span beams with varying sections

4.2.1 Example 1: non-prismatic beam

The first example is a single-span beam whose section is non-prismatic. The depth of each element is randomly generated to have the Gaussian distribution whose mean is 0.004 m (i.e., the original depth) and standard deviation is 0.0008 m. Fig. 6 shows the graphical representation of the generated non-prismatic beam. Dashed line represents the original depth for visual comparison.

Fig. 7 shows the first three mode shapes of the model compared with the assumed sinusoidal mode shapes. The assumed mode shapes are almost identical to the actual mode shapes, as quantified by the MAC (modal assurance criterion) values close to unity, despite of the sectional variation. Therefore, the modal mapping matrix D using the assumed mode shapes is expected to be slightly different with the exact matrix.

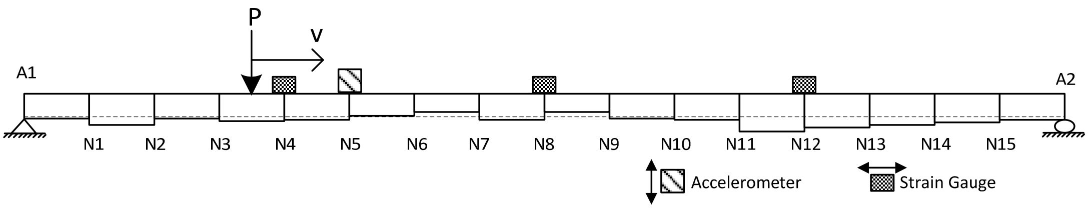

Fig. 6 Example 1 – Non-prismatic single-span beam model

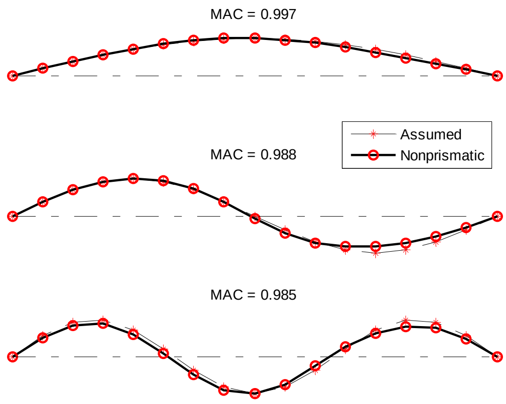

Fig. 7 Example 1 – first three mode shapes compared with assumed ones

Using the simulated acceleration at N5 and strains at N4, N8, and N12, the displacements at N5 are estimated by the three indirect methods introduced in Section 2 and compared with the exact displacement. Fig. 8 is the comparison of the estimated displacements at node N5 by the three indirect methods, introduced in Section 2, with exact displacement. The acceleration-based method (see Fig. 8(a)) accurately estimates the high-frequency component of the displacement, as clearly shown in the zero-mean tail part (after 15 sec). However, the method cannot estimate the low-frequency (i.e., quasi-static) component that is generated when the directional loading (e.g., vehicle loading) is applied. Meanwhile, the strain-based method (see Fig. 8(b)) estimates the low-frequency component of the displacement while missing the high-frequency component. The IDEAS method (see Fig. 8(c)) estimates almost identical displacement to the exact displacement.

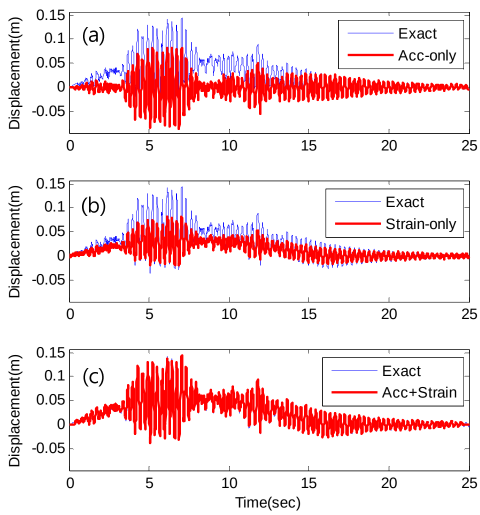

Fig. 8 Example 1 – comparison of time-domain displacements estimated at N5: (a) acceleration-based method, (b) strain-based method, and (c) IDEAS method

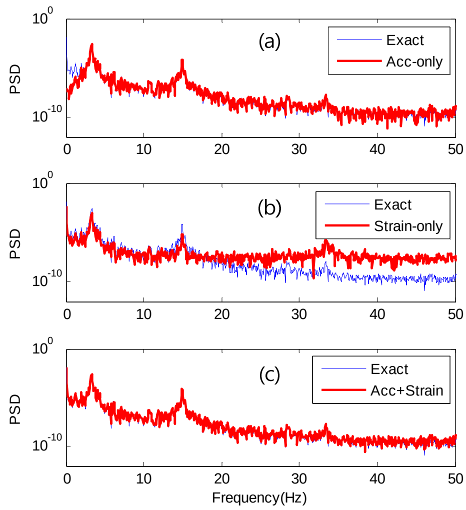

Fig. 9 Example 1 – comparison of PSDs of estimated displacements at N5: (a) acceleration-based method, (b) strain-based method, and (c) IDEAS method

Fig. 9 shows the power spectral densities (PSD) of the estimated displacements compared to the PSD of the exact displacement. The PSD from the acceleration-based method is almost identical to the exact PSD except very low-frequency range below 2 Hz. The PSD from the strain-based method is relatively close to the PSD of the exact displacement, while the high-frequency component above 15 Hz differs from the exact PSD. The IDEAS method shows almost identical PSD to the exact one. This result demonstrates that the IDEAS method makes a synergic use of both of the methods by the fusion of acceleration and strain data.

4.2.2 Example 2: asymmetric beam

The second example is a single-span beam whose section is asymmetric as shown in Fig.10. The depths of the right-half span (from N8 to A2) are decreased to 0.002 m, which is a half of the original depth (i.e., 0.004 m). The simulation setup is exactly same as the previous non-prismatic beam example. Fig. 11 shows the first three mode shapes of the model compared with the assumed mode shapes. The assumed modes show big discrepancies with the actual mode shapes of the model, which is also quantified with the low MAC values. Therefore, the modal mapping matrix D, composed using the assumed modes, cannot be expected to map the strain to the displacement with high accuracy.

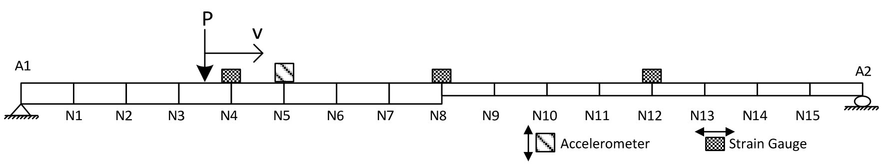

Fig. 10 Example 2 – asymmetric single-span beam model

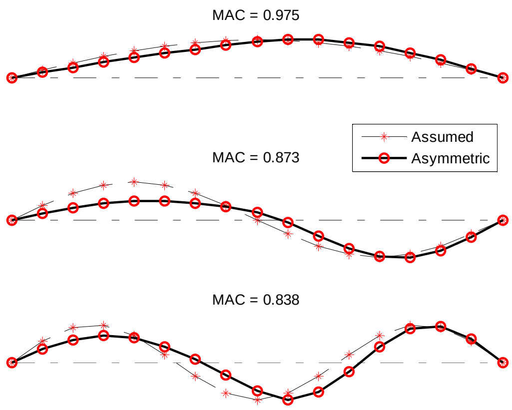

Fig. 11 Example 2 – first three mode shapes compared with assumed ones

Fig. 12 is the comparison of the estimated displacements with exact displacement. In the case of strain-based method, the displacement is badly estimated as expected due to the significant discrepancy between the assumed modes and actual modes. The IDEAS method shows larger error than Fig. 8, but still estimates the displacement with higher accuracy than the other methods. Fig. 13 shows the comparison in the frequency domain. By using both of the acceleration and strain, the IDEAS method provides better estimates in the high frequency range than the acceleration-based method and in the low frequency range than the strain-based method. The result shows that the fusion of two responses which have strengths in different frequency ranges provides the robustness to the measurement noise as well as the big discrepancy of the assumed modes.

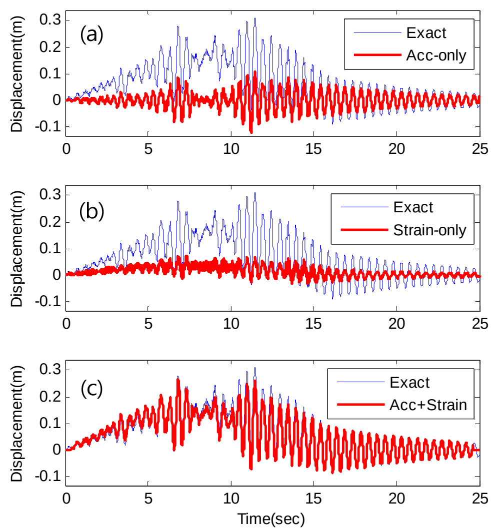

Fig. 12 Example 2 – comparison of time-domain displacements estimated at N5: (a) acceleration-based method, (b) strain-based method, and (c) IDEAS method

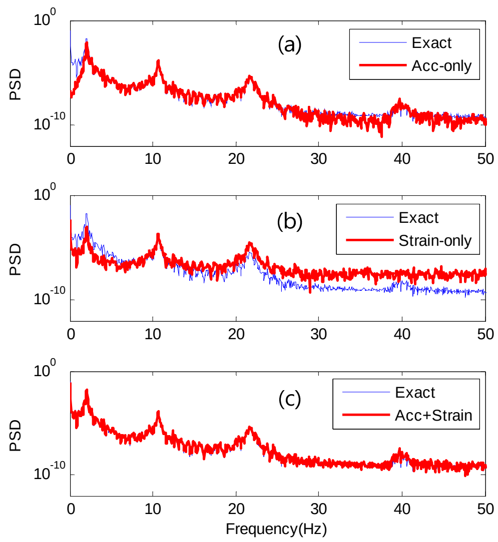

Fig. 13 Example 2 – comparison of PSDs of estimated displacements at N5: (a) acceleration-based method, (b) strain-based method, and (c) IDEAS method

4.3 Multi-span beams

4.3.1 Example 3: two-span prismatic beam

The third example is the two-span prismatic beam shown in Fig. 14. The second span is the duplicate of the single-span prismatic beam model shown in Fig. 4. The two-span model is selected as an example since the multi-span model has multiple modes that have similar mode shapes for a single span (e.g., from A1 to A2) by the action of the extended spans. Fig. 15 shows the first six mode shapes of the two-span model compared with the assumed mode shapes for a single span. By looking at the first single span, the similar mode shapes are repeated twice with some difference due to the action of the intermediate support A2. The odd orders of modes have identical shapes to the assumed mode shapes as indicated by the MAC values of unity, while the even orders of modes have slightly different shapes with smaller MAC values.

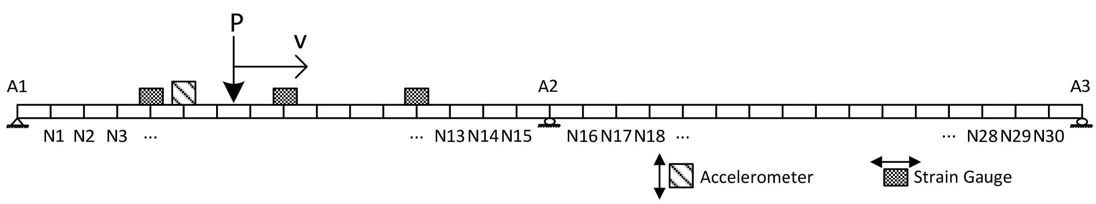

Fig. 14 Example 3 – two-span prismatic beam model

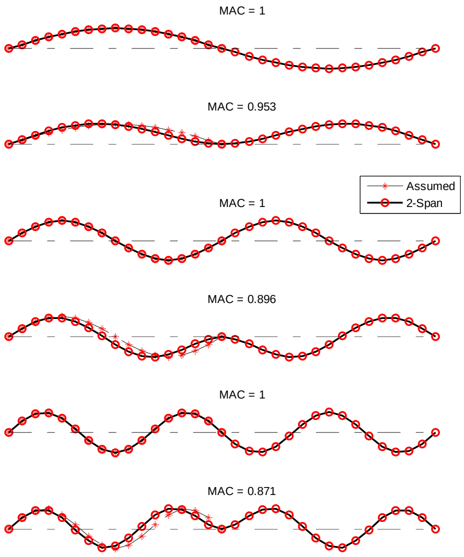

Fig. 15 Example 3 – first six mode shapes compared with assumed ones

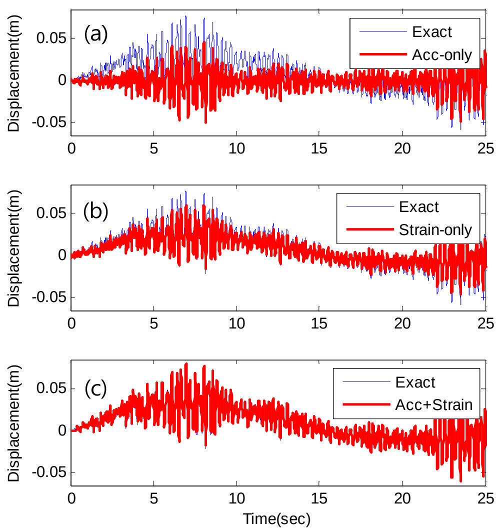

Fig. 16 Example 3 – comparison of time-domain displacements estimated at N5: (a) acceleration-based method (b) strain-based method, and (c) IDEAS method

Figs. 16 and 17 are the comparison of the estimated displacements with exact displacement in the time and frequency domain, respectively, and they show the aforementioned benefit clearly. Similar to the previous results, the two previous methods showed big discrepancy in either low-frequency range or high-frequency range. The IDEAS method estimates the dynamic displacement with negligible error, though the even orders of modes show the low MAC values comparable with the MAC values of Example 2 shown in Fig. 11. In the frequency-domain, the six peaks of the exact PSD are tracked well by the PSD of the estimated displacement using the mapping matrix composed of using only three assumed modes. Considering that the IDEAS method showed visible error in time-domain (though it was insignificant) in Example 2, this result shows substantial robustness to the increasing spans.

4.3.2 Example 4: two-span beam with asymmetric sections

The fourth example is the two-span prismatic beam similar to the Example 3, but having asymmetric sections for each span as shown in Fig. 18. The second span (i.e., from A2 to A3) is designed to have the depth which is a half of the first span, while keeping the other parameters. Fig. 19 shows the first seven mode shapes of the two-span model compared with the assumed mode shapes for a single span. Contrast to the previous two-span model, this model has seven modes which has similar mode shapes to the first three sinusoidal modes. Looking at the first single span, the mode sequence correlated to the assumed modes is changed from the previous model: the first and second modes are correlated to the first sinusoidal mode, the third, fourth, and fifth modes are to the second sinusoidal mode, and the other two modes are to the third sinusoidal mode. Especially, the third mode with a relatively low MAC value (close to 0.5) occurred by the weaker second span, while keeping the other modes shown in Fig. 15.

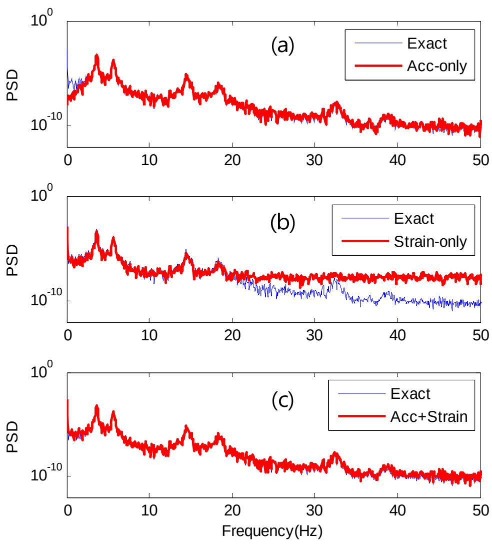

Fig. 17 Example 3 – comparison of time-domain displacements estimated at N5: (a) acceleration-based method, (b) strain-based method, and (c) IDEAS method

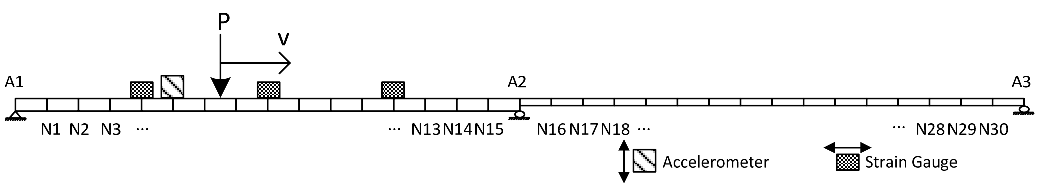

Fig. 18 Example 4 – two-span beam model with asymmetric sections

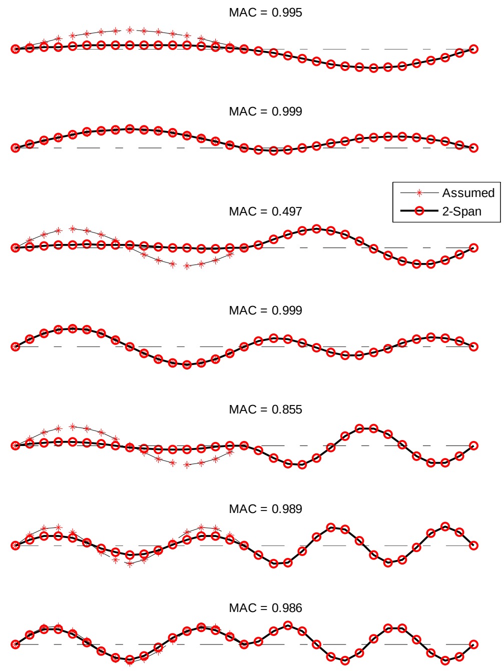

Fig. 19 Example 4 – first seven mode shapes compared with assumed ones

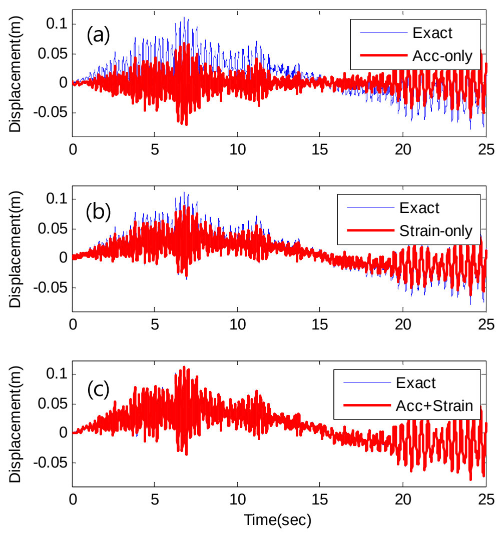

Fig. 20 Example 4 – comparison of time-domain displacements estimated at N5: (a) acceleration-based method, (b) strain-based method, and (c) IDEAS method

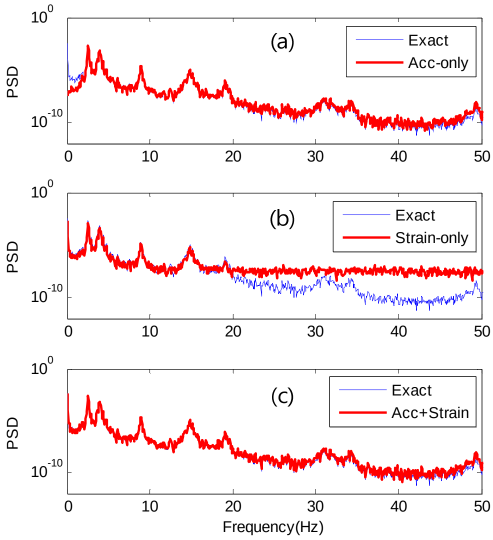

Fig. 21 Example 4 – comparison of PSDs of estimated displacements at N5: (a) acceleration-based method, (b) strain-based method, and (c) IDEAS method

Figs. 20 and 21 are the comparison of the estimated displacements with exact displacement in the time and frequency domain, respectively. The IDEAS method estimates the dynamic displacement with negligible error in both time and frequency domain despite of the third mode with very low MAC value. The seven peaks of the exact PSD are tracked well by the PSD of the estimated displacement using the mapping matrix composed of using only three assumed modes, while the eighth peak at 49 Hz is not. One thing to note is that the third mode is also tracked very well despite of its low MAC value of 0.5.

The result of this simulation can be extended to the beams with more than two spans. The action of the multiple spans will generate more number of modes whose mode shapes are similar to several lower sinusoidal shapes. Some of them will have very similar mode shapes to the assumed ones for a *monitoring span* and the others will not. Regardless of the correlation (i.e., MAC value) of the appeared modes, all the modes which have somewhat similarity to the three assumed modes will be considered in constructing the modal mapping matrix as shown in Fig. 19. This brings a big benefit in estimating the accurate displacement of a single span while keeping the number of strain gauges as three, and the benefit will appear larger for the beams with more spans.

5. Conclusions

In this paper, the indirect displacement estimation using acceleration and strain (IDEAS) method has been extended to various beam-type structures beyond the previous validation on the prismatic or near-prismatic beams done by Park *et al.* (2013). In this paper, the extension to the general types of beams has been verified by the mathematical formulation of modal mapping matrix using the sinusoidal mode shapes. By constructing the modal mapping matrix only for the monitored substructure, so-called *monitoring span* in this paper, it has been demonstrated that only a few sinusoidal assumed mode shapes acts for the repeated mode shapes on the *monitoring span*, which appear on the continuous beams and wide beams. The effect of disagreement of the assumed mode shapes to the actual mode shapes has been investigated from the numerical simulation of four types of beams: a single-span beam with non-prismatic section, a single-span beam with asymmetric section, a two-span beam with prismatic section, and a two-span beam with asymmetric sections. By forcing a moving load, the displacements estimated by the IDEAS method on the four numerical models are compared with the exact displacements as well as the ones estimated displacements by the acceleration-based and strain-based methods in time and frequency domains. The results of the numerical validation can be summarized as:

(1) For single-span beams, the sectional irregularities of numerical models rarely affect the accuracy of the displacement estimation by the IDEAS method that has better accuracy than the acceleration-based and strain-based method.
(2) For 2-span continuous beams, the IDEAS method still works accurately using a few sinusoidal assumed mode shapes by introducing the concept of *monitoring span*, which allows the extension of the IDEAS method to continuous beams with multiple-spans.
(3) The comparison in the frequency domain shows that the displacements estimated by the IDEAS method is precise at both low- and high-frequency ranges for all types of beams.

The results of this study evidence the applicability of the IDEAS method to effectively measure the displacements of the beam-type structures where the direct measurements are not available, such as bridges crossing straits, rivers, narrows, or highways.

Acknowledgements

This research was supported by a grant(13SCIPA01) from Smart Civil Infrastructure Research Program funded by Ministry of Land, Infrastructure and Transport(MOLIT) of Korea government and Korea Agency for Infrastructure Technology Advancement(KAIA).

References

Altunisik, A.C., Bayraktar, A. and Ozdemir, H. (2012), "Seismic safety assessment of eynel highway steel bridge using ambient vibration measurements", *Smart Struct. Syst.*, **10**(2), 131-154.

Atkinson, K.E. (2008), *An introduction to numerical analysis*, John Wiley & Sons.

Bani-Hani, K.A., Zibdeh, H.S. and Hamdaoui, K. (2008), "Health monitoring of a historical monument in Jordan based on ambient vibration test", *Smart Struct. Syst.*, **4**(2), 195-208.

Doebling, S.W., Farrar, C.R. and Prime, M.B. (1998), "A summary review of vibration-based damage identification methods", *Shock Vib. Digest*, **30**, 91-105.

Foss, G. and Haugse, E. (1995), "Using modal test results to develop strain to displacement transformations", *Proceedings of the 13th Int. Modal Analysis Conf.*

Gindy, M., Nassif, H.H. and Velde, J. (2008), "Bridge displacement estimates from measured acceleration records", *Transport. Res. Rec.*, **2028**, 136-145.

Jung, B.S., Kim, N.S. and Koon, S.K. (2006), "Estimation of displacement responses using the wavelet decomposition signal", *J. Korea Concrete Inst.*, **18**(3), 347-354.

Kandula, V., DeBrunner, L., DeBrunner, V. and Rambo-Roddenberry, M. (2012), "Field testing of indirect displacement estimation using accelerometers", *Proceedings of the Conf. Record of the 46th Asilomar Conf. Signals, Systems, and Computers*.

Kang, L.H., Kim, D.K. and Han, J.H. (2007), "Estimation of dynamic structural displacements using fiber Bragg grating strain sensors", *J. Sound Vib.*, **305**(3), 534-542.

Koo, K.Y., Sung, S.H., Park, J.W. and Jung, H.J. (2010), "Damage detection of shear buildings using deflections obtained by modal flexibility", *Smart Mat. Struct.*, **19**(11), 115026.

Kim, J.T., Ho, D.D., Nguyen, K.D., Hong, D.S., Shin, S.W., Yun, C.B. and Shinozuka, M. (2013), "System identification of a cable-stayed bridge using vibration responses measured by a wireless sensor network", *Smart Struct. Syst.*, **11**(5), 533-553.

Lee, J.J. and Shinozuka, M. (2006), "A vision-based system for remote sensing of bridge displacement", *NDT & E Int.*, **39**(5), 425-431.

Lee, H.S., Hong, Y.H. and Park, H.W. (2010), "Design of an FIR filter for the displacement reconstruction using measured acceleration in low-frequency dominant structures", *Int. J. Numer. Meth. Eng.*, **82**(4), 403-434.

Ma, T.W., Bell, M., Lu, W. and Xu, N.S. (2014), "Recovering structural displacements and velocities from acceleration", *Smart Struct. Syst.*, **14**(2), 191-207.

Nassif, H.H., Gindy, M. and Davis, J.(2005), "Comparison of laser Doppler vibrometer with contact sensors for monitoring bridge deflection and vibration", *NDT & E Int.*, **38**(3), 213-218.

Park, J.W., Sim, S.H. and Jung, H.J. (2013), "Displacement estimation using multimetric data fusion", *IEEE/ASME Trans. Mechatronics*, **18**(6), DOI: 10.1109/TMECH.2013.2275187.

Park, K.T., Kim, S.H., Park, H.S. and Lee, K.W. (2005), "The determination of bridge displacement using measured acceleration", *Eng. Struct.*, **27**(3), 371-378.

Ribeiro, J.G.T., Freire, J.L.F. and Castro, J.T.P. (1997), "Problems in analogue double integration to determine displacements from acceleration data", *Proceedings of the 15th Int. Modal Anal. Conf.*

Shin, S., Lee, S.U. and Kim, N.S. (2012), "Estimation of bridge displacement responses using FBG sensors and theoretical mode shapes," *Struct. Eng. Mech.*, **42**(2), 229-245.

Ye, X.W., Ni, Y.Q., Wai, T.T., Wong, K.Y., Zhang, X.M. and Xu, F. (2013)."A vision-based system for dynamic displacement measurement of long-span bridges: algorithm and verification", *Smart Struct. Syst.*, **12**(3-4), 363-379.

Yi, J.H., Cho, S., Koo, K.Y., Yun, C.B., Kim, J.T., Lee, C.G. and Lee, W.T. (2007), "Structural performance evaluation of a steel-plate girder bridge using ambient acceleration measurements", *Smart Struct. Syst.*, **3**(3), 281-298.

Zhou, C., Li, H.N., Li, D.S., Lin, Y.X. and Yi, T.H. (2013), "Online damage detection using pair cointegration method of time-varying displacement", *Smart Struct. Syst.*, **12**(3-4), 309-325.

CY